Hydrodynamic Model Description

Cairidh & Maol Ban, Caol Mor

CAR/L/1010432 & CAR/L/1009643

September 2025

Mowi Scotland

OFFICE
Mowi, Farms Office, Glen Nevis Business Park
PH33 6RX Fort William

POSTAL
Mowi, Farms Office, Glen Nevis Business Park
PH33 6RX Fort William

PHONE

FAX
-

MAIL
environment@mowi.com

WEB
http://mowiscotland.co.uk

CONTENTS

LIST OF FIGURES

LIST OF TABLES

1. Introduction

This report has been prepared by Mowi Scotland Ltd. to meet the requirements of the Scottish Environment Protection Agency (SEPA) for an application to increase the consent of topical sealice veterinary medicines at the **Cairidh and Maol Ban** marine salmon farms in the **Caol Mor** region of Skye (Figure 1). The application uses coupled hydrodynamic and particle tracking modelling to describe the dispersion of bath treatments in order to determine EQS-compliant quantities for the current sites' biomass and equipment. The modelling procedure follows as far as possible guidance presented by SEPA in December 2023 (SEPA, 2023). This report describes the configuration, calibration and validation of the hydrodynamic model used in the applications. The bath dispersion modelling for the two sites is described in separate reports (Mowi, 2025a, 2025b).

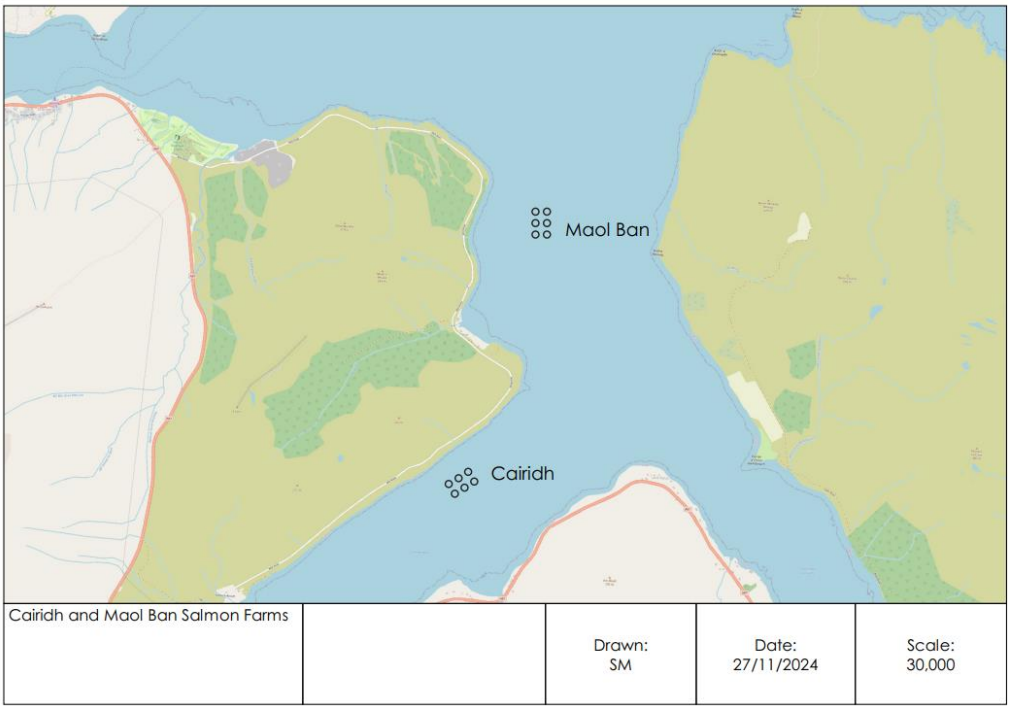

Figure 1. Cairidh and Maol Ban salmon farm locations. Current meter deployment locations are indicated by black triangles

2. Configuration and Boundary Forcing

The hydrodynamic modelling was performed using the RiCOM (River and Coastal Ocean Model; Walters and Casulli, 1998). The unstructured mesh used in the modelling (Figure 2) was adapted from the East Coast of Lewis and Harris (ECLH) sub-model mesh of the Scottish Shelf Model (SSM; Marine Scotland, 2016). The model resolution was enhanced in the Caol Mor region, particularly around the Cairidh and Maol Ban sites (Figure 3). The spatial resolution of the model varied from 20 m in some inshore waters and round the farm pens to 5 km along the open boundary. The model consisted of 55,208 nodes and 103,959 triangular elements. Model bathymetry (Figure 4) was also taken from the ECLH sub-model (SSM, MS 2016).

The model was forced along its open boundary by eight tidal constituents (M_2, S_2, N_2, K_2, O_1, K_1, P_1 and Q_1) taken from the full Marine Scotland Scottish Shelf Model (SSM; Marine Scotland, 2016) using the MATLAB© tidal analysis routine t_tide (Pawlowicz et al., 2002). Wind speed and direction data were taken from the European Centre for Medium-Range Weather Forecasts (ECMWF 2021), with data interpolated onto the nodal locations of the model mesh.

The model was run in 3D, with 15 sigma layers in the vertical. The sigma levels were closer together near the surface and seabed, with sigma level depths of: σ = [0 -0.02 -0.04 -0.06 -0.10 -0.20 -0.30 -0.40 -0.50 -0.60 -0.70 -0.80 -0.90 -0.95 -1.0]. Freshwater discharges were input to the model domain at 155 locations, with the freshwater flux data at each location based on the climatological river flows from the Scottish Shelf Model. Initial 3D density fields for the start of the simulation were derived from the Scottish Shelf Model temperature and salinity fields for the corresponding start day.

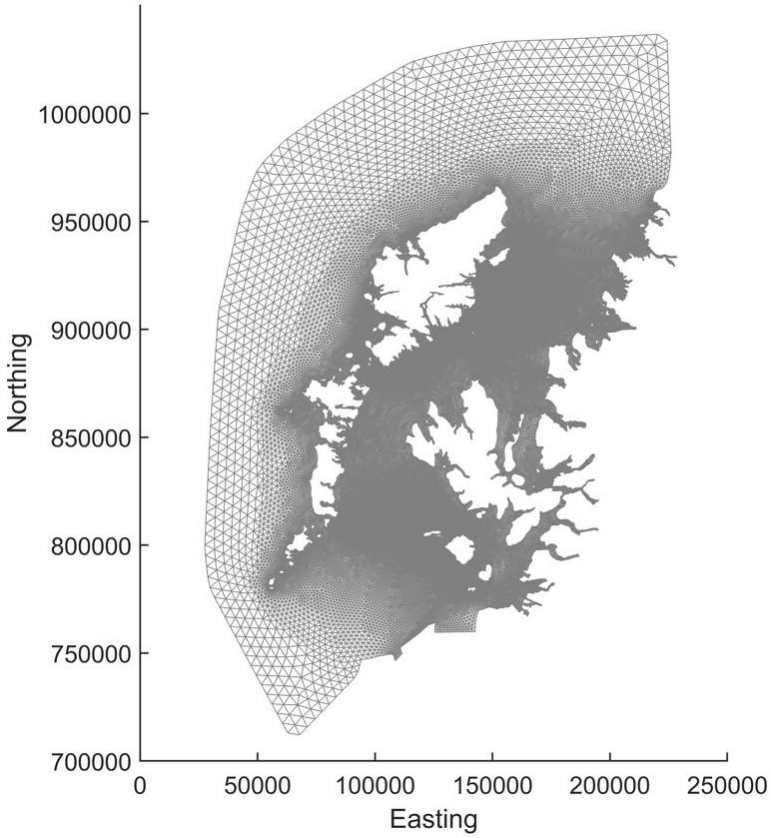

Figure 2. The ECLH mesh and domain of the modelling study (SSM)

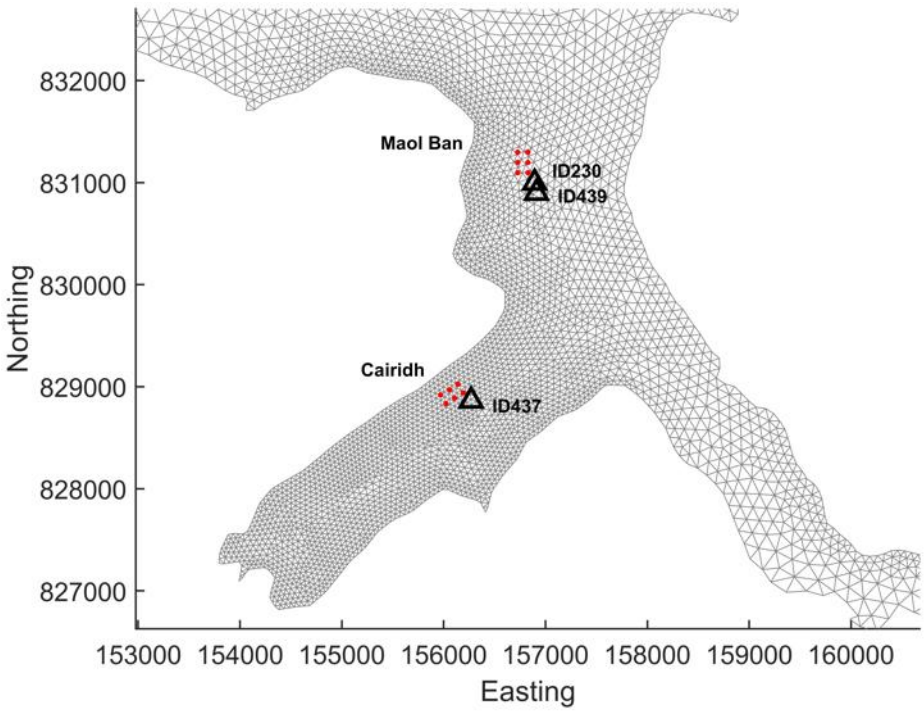

Figure 3. The unstructured mesh around the Cairidh and Maol Ban sites in the modified model grid, with the pen locations indicated (*).

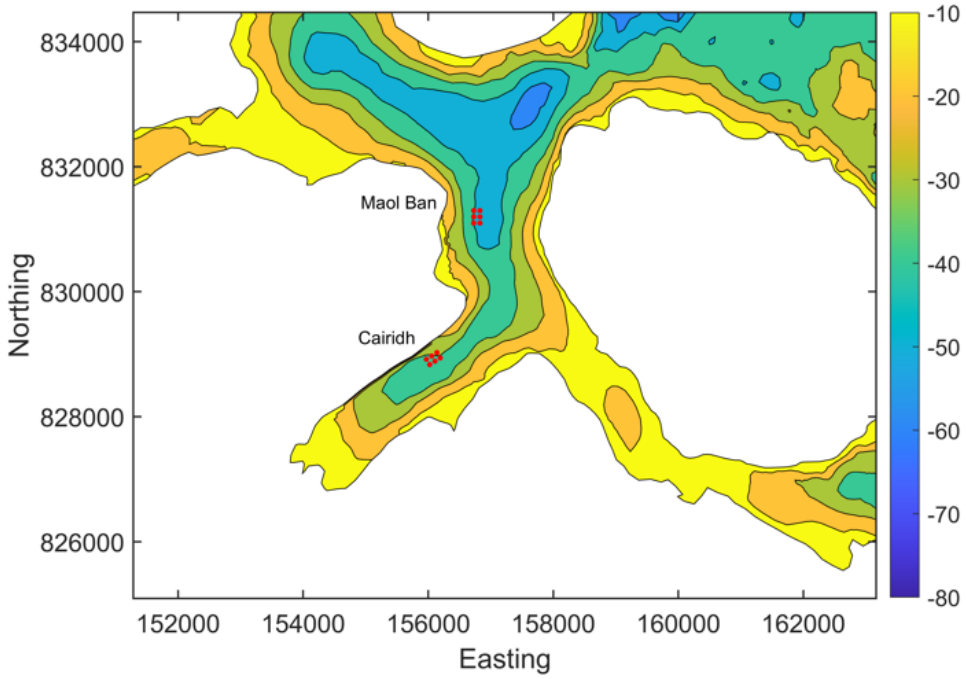

Figure 4. Model water depths (m) in the area around the Cairidh and Maol Ban salmon farms. The pen locations are indicated (●).

3. Model Calibration and Validation with Hydrographic Data

For the current study, the RiCOM model was calibrated against hydrographic data collected in the region of the Cairidh farm site and the neighboring Maol Ban site in 2024. The data are described in the relevant hydrographic reports. In March 2024, a Nortek Signature 1000 ADCP instrument was deployed close to the Cairidh site until June 2024 (ID437). In June 2024 the same instrument was then re-deployed close to the neighboring Maol Ban site until August 2024 (ID439). In 2018, a standard ADCP was deployed (ID230) from July until September. In all, 206 days of current data were used in this application. The ADCP deployments provided both current velocity and seabed pressure data, which were used to calibrate and validate modelled velocity and sea surface height. The model was calibrated initially against data from March - June 2024 (ID437), then validated against data from the other deployment, ID439.

For each simulation, the model was “spun-up” for seven days with boundary forcing ramped up from zero over a period of 48 hours. The model state at the end of the 168-hour spin-up period was stored, and the main simulations “hot-started” from this state.

The following main simulations were performed, corresponding with the dates of the ADCP deployments:

(i) Calibration: Cairidh, March 2024 – June 2024 (ID437)
(ii) Validation: Maol Ban June 2024 – August 2024 (ID439)
(iii) Validation: Maol Ban, July 2018 – September 2018 (ID230)

[Note that the dates above refer to the main simulations and that the spin-up simulations ran for seven days prior to the start dates given above.]

Model performance is assessed using three metrics: the mean absolute error (MAE), the root-mean-square error (RMSE) and the model skill (d_2). The first two are standard measures of model accuracy; the third, d_2, is taken from Willmott et al. (1985) and lies in the range $0 \leq d_2 \leq 1$, with $d_2 = 0$ implying zero model skill and $d_2 = 1$ indicating perfect skill.

3.1 Calibration: March – June 2024, ID437

The calibration used observed depth and current velocity from the ADCP location to compare with modelled sea surface height (SSH) and velocity. The model was calibrated by varying the value of the bed roughness coefficient, z_0, which determines the frictional effect of the seabed on the flow, and the surface roughness length scale, zs. After a number of simulations, a final parameter set was selected (Table 1).

Table 1. Parameter values chosen for the RiCOM model during the calibration simulations.

Parameter Description	Value
Drag coefficient, C_D	0.01
Number of vertical levels	15
Model time step (s)	72

The results of the calibration exercise are presented in Figure 9 – Figure 12 and Table 3. At the ADCP location, the sea surface height was reasonably accurately modelled, with model

skill of 0.99. The mean absolute error (MAE) and root-mean-square error (RMSE) values of 0.14 m and 0.18 m are about 2.8 % and 3.6 % of the spring tide range (5 m) respectively.

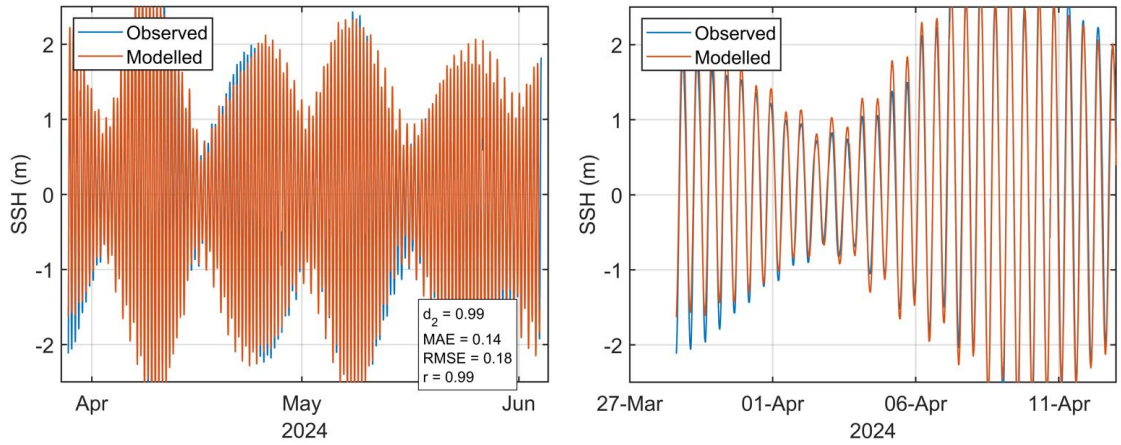

Figure 5. Comparison between observed and modelled sea surface height from March – June 2024 (ADCP deployment ID437) using model parameter values from Table 1. Both the full record (left) and a subset of 15 days (right) are shown. Observed data are in blue, model results in red.

For the calibration period, the model skill scores for the East component were 0.61, 0.59 and 0.53 at the three selected cell depths. For the North component of velocity, the model skill scores were 0.57, 0.52 and 0.54 at the three selected cell depths. MAE and RMSE values were between 0.02 and 0.04 for the two velocity components at the three cell depths (Table 3, Figure 10). The scatter plots and histograms demonstrate that the modelled current had broadly the same magnitude and direction characteristics as the observed data (Figure 11 and Figure 12).

Table 2. Model performance statistics for East and North velocity at the ADCP location from March - June 2024 (ID437) for the three selected cells.

		East	North
Near-surface cell	Model skill	0.61	0.57
	MAE	0.04	0.03
	RMSE	0.05	0.04
Cage-bottom cell	Model skill	0.59	0.52
	MAE	0.03	0.03
	RMSE	0.04	0.03
Near-bed cell	Model Skill	0.53	0.54
	MAE	0.03	0.02
	RMSE	0.04	0.03

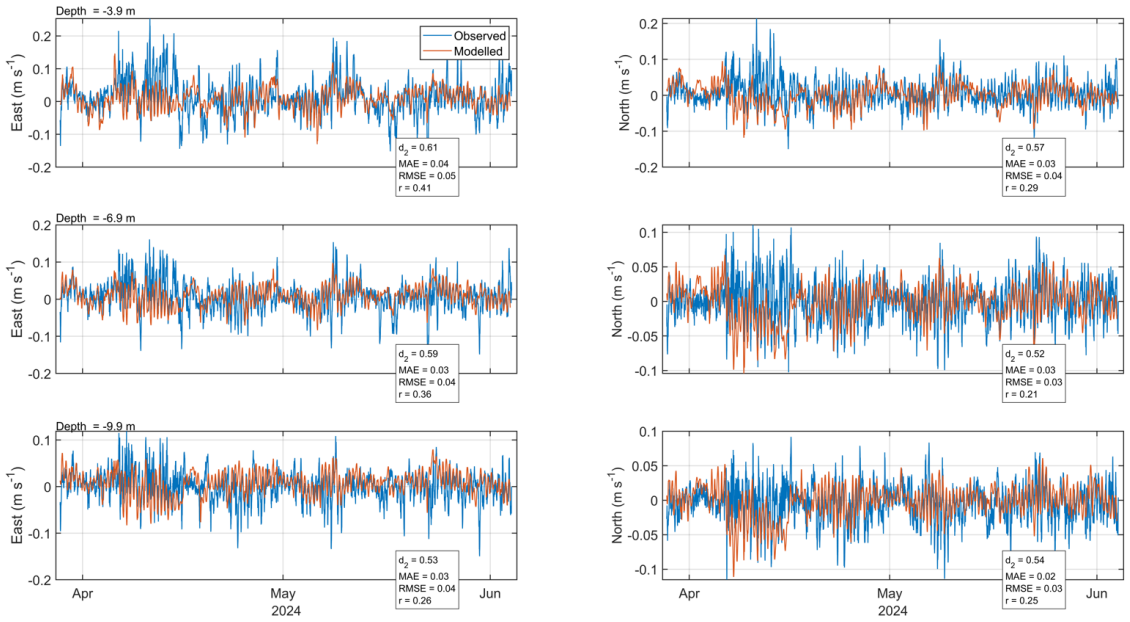

Figure 6. Comparison between observed and modelled East (left) and North (right) components of velocity at the three selected cell depths at the ADCP location for 15 days in March - June 2024 (ID437). Observed data are in blue, model results in red.

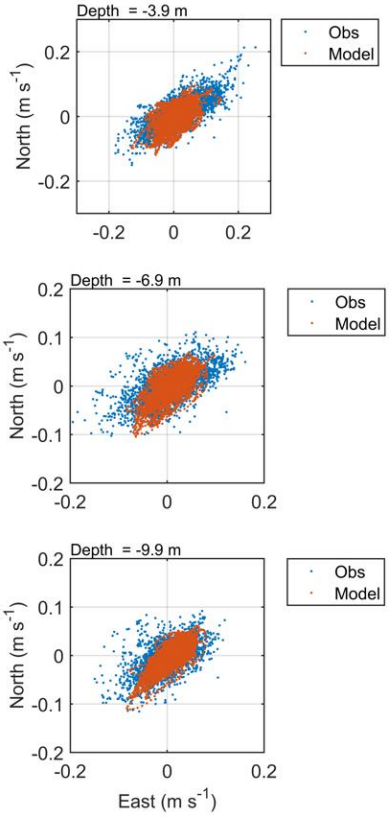

Figure 7. Scatter plot of observed and modelled velocity at each of the three selected cell depths at the ADCP location from March - June 2024 (ID437). Observed data are in blue, model results in red.

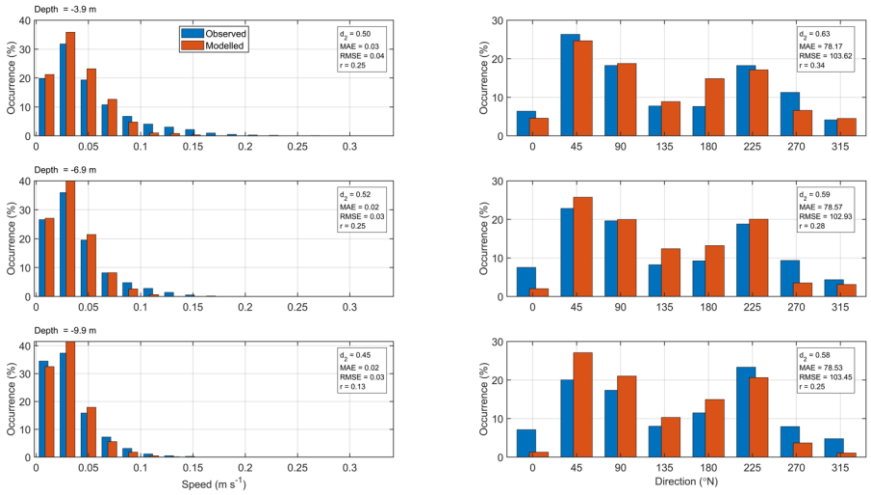

Figure 8. Histograms of observed and modelled speed (left) and direction (right) at the three selected cell depths at the ADCP location from March - June 2024 (ID437). Observed data are in blue, model results in red.

3.2 Validation: June – August 2024, ID439

The model was then validated using the data collected at the near-by Maol Ban site in June 2024. It used observed depth and current velocity from the ADCP location to compare with modelled sea surface height (SSH) and velocity. The model was validated by using the same parameters as above.

The results of the validation exercise are presented in Figure 9 – Figure 12 and Table 3. At the ADCP location, the sea surface height was reasonably accurately modelled, with model skill of 1. The mean absolute error (MAE) and root-mean-square error (RMSE) values of 0.12 m and 0.14 m are about 2.4 % and 2.8 % of the spring tide range (5.0 m) respectively.

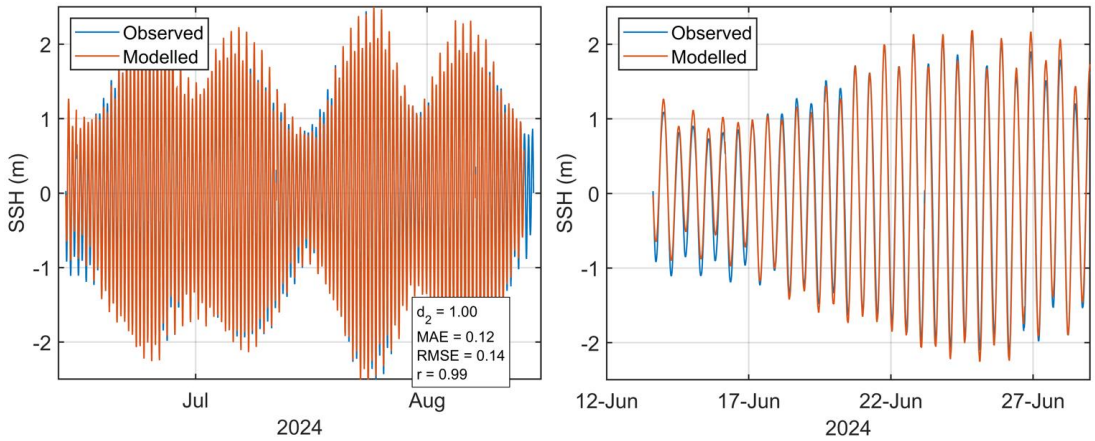

Figure 9. Comparison between observed and modelled sea surface height from June - August 2024 (ADCP deployment ID439) using model parameter values from Table 1. Both the full record (left) and a subset of 15 days (right) are shown. Observed data are in blue, model results in red.

For the calibration period, the model skill scores for the East component were 0.30, 0.32 and 0.35 at the three selected cell depths. For the North component of velocity, the model skill scores were 0.65, 0.65 and 0.68 at the three selected cell depths. MAE and RMSE values were between 0.03 and 0.09 for the two velocity components at the three cell depths (Table 3, Figure 10). The scatter plots and histograms demonstrate that the modelled current had broadly the same magnitude and direction characteristics as the observed data (Figure 11 and Figure 12). The modelled near-bed currents are weaker than the observed, but since bath medicine dispersion occurs in the near-surface layers, where the comparison was better, the weaker near-bed currents are unlikely to impact the bath medicine dispersion simulations.

Table 3. Model performance statistics for East and North velocity at the ADCP location from June - August (ID439) for the three selected cells.

		East	North
Near-surface cell	Model skill	0.30	0.71
	MAE	0.04	0.06
	RMSE	0.05	0.08
Cage-bottom cell	Model skill	0.27	0.71
	MAE	0.03	0.05
	RMSE	0.05	0.07
Near-bed cell	Model Skill	0.32	0.70
	MAE	0.03	0.04
	RMSE	0.04	0.06

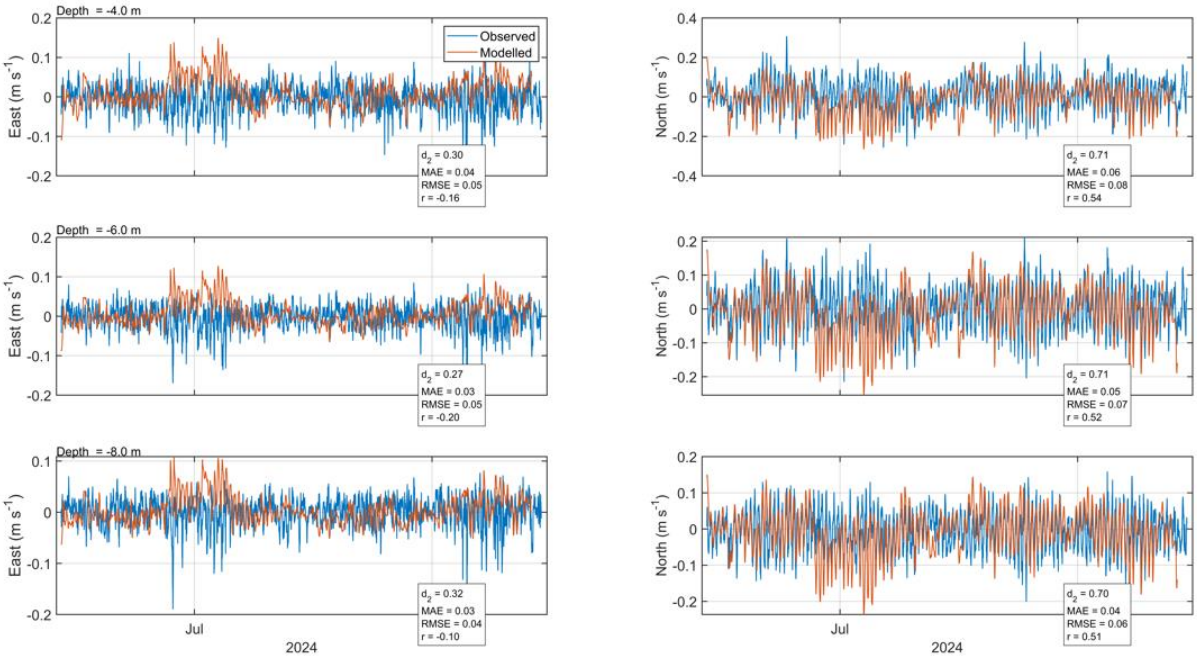

Figure 10. Comparison between observed and modelled East (left) and North (right) components of velocity at the three selected cell depths at the ADCP location for 15 days in June - August 2024 (ID439). Observed data are in blue, model results in red.

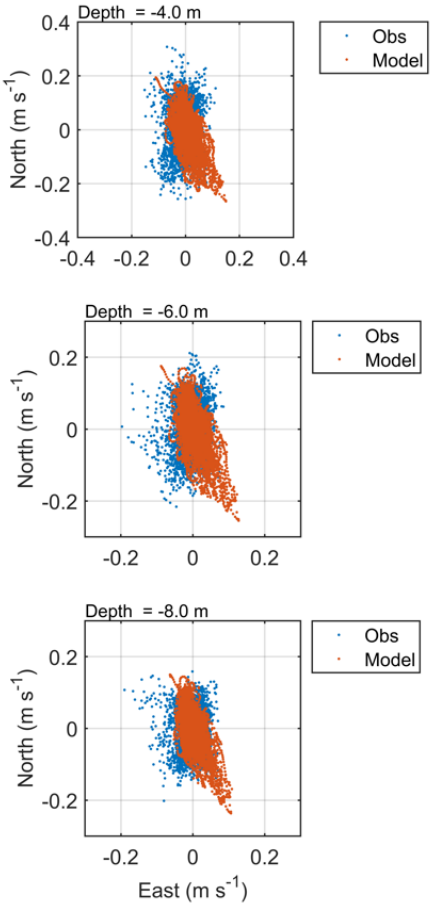

Figure 11. Scatter plot of observed and modelled velocity at each of the three selected cell depths at the ADCP location from June - August 2024 (ID439). Observed data are in blue, model results in red.

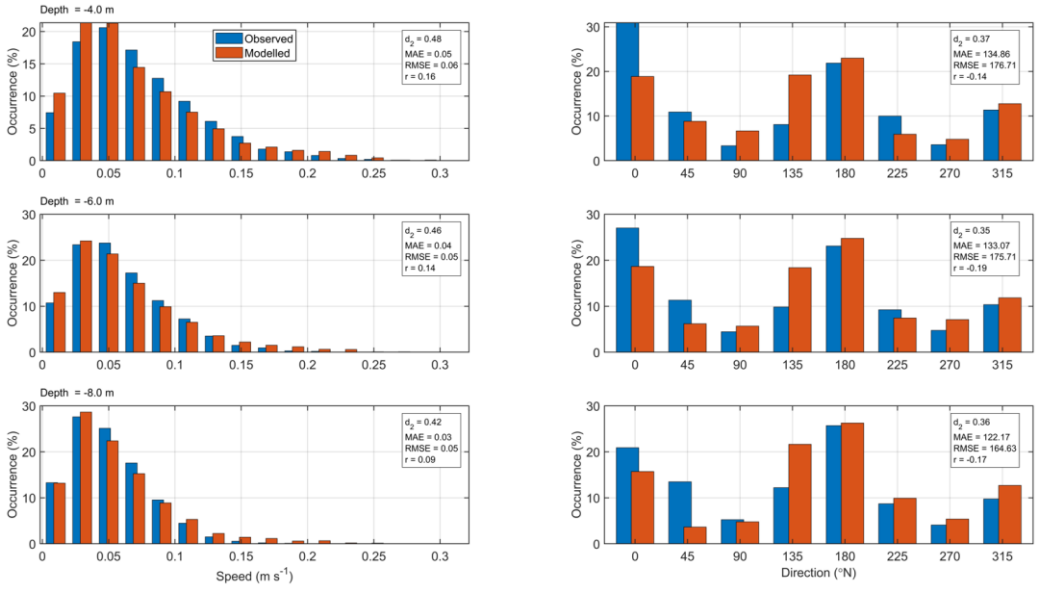

Figure 12. Histograms of observed and modelled speed (left) and direction (right) at the three selected cell depths at the ADCP location from June – August 2024 (ID439). Observed data are in blue, model results in red.

3.3 Validation: July – September 2018, ID230

The model was then validated again using the data collected at the near-by Maol Ban site in July 2018. It used observed depth and current velocity from the ADCP location to compare with modelled sea surface height (SSH) and velocity. The model was validated again by using the same parameters as above.

The results of the validation exercise are presented in Figure 13 - Figure 16 and Table 4. At the ADCP location, the sea surface height was reasonably accurately modelled, with model skill of 1. The mean absolute error (MAE) and root-mean-square error (RMSE) values of 0.12 m and 0.14 m are about 2.4 % and 2.8 % of the spring tide range (5.0 m) respectively.

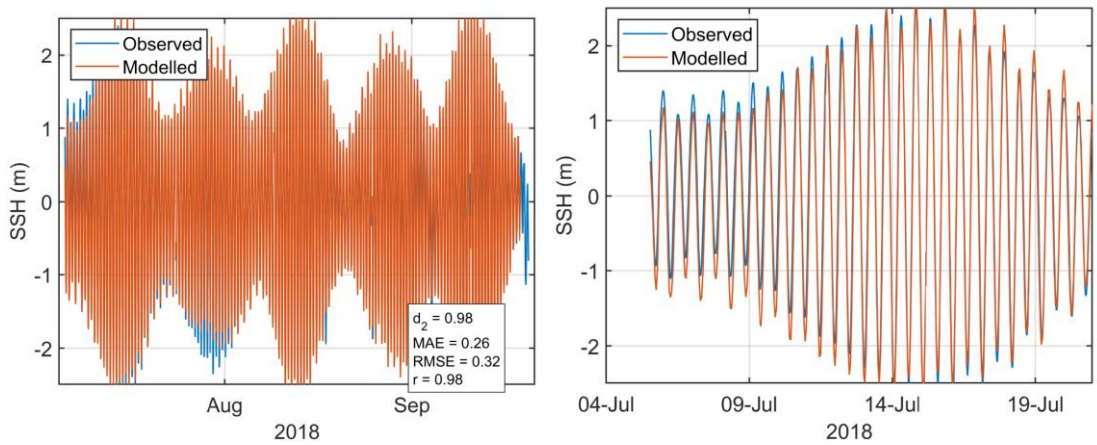

Figure 13. Comparison between observed and modelled sea surface height from July - September 2018 (ADCP deployment ID230) using model parameter values fromTable 1. Both the full record (left) and a subset of 15 days (right) are shown. Observed data are in blue, model results in red.

For the validation period, the model skill scores for the East component were 0.43, 0.46 and 0.34 at the three selected cell depths. For the North component of velocity, the model skill scores were 0.74, 0.75 and 0.53 at the three selected cell depths. MAE and RMSE values were between 0.02 and 0.06 for the two velocity components at the three cell depths (Table 3, Figure 10). The scatter plots and histograms demonstrate that the modelled current had broadly the same magnitude and direction characteristics as the observed data (Figure 11 and Figure 12). The modelled near-bed currents are weaker than the observed, but since bath medicine dispersion occurs in the near-surface layers, where the comparison was better, the weaker near-bed currents are unlikely to impact the bath medicine dispersion simulations.

Table 4. Model performance statistics for East and North velocity at the ADCP location from July – September 2018 (ID230) for the three selected cells.

		East	North
Near-surface cell	Model skill	0.43	0.74
	MAE	0.03	0.05
	RMSE	0.04	0.06
Cage-bottom cell	Model skill	0.46	0.75
	MAE	0.02	0.04
	RMSE	0.03	0.05
Near-bed cell	Model Skill	0.34	0.53
	MAE	0.03	0.05
	RMSE	0.04	0.06

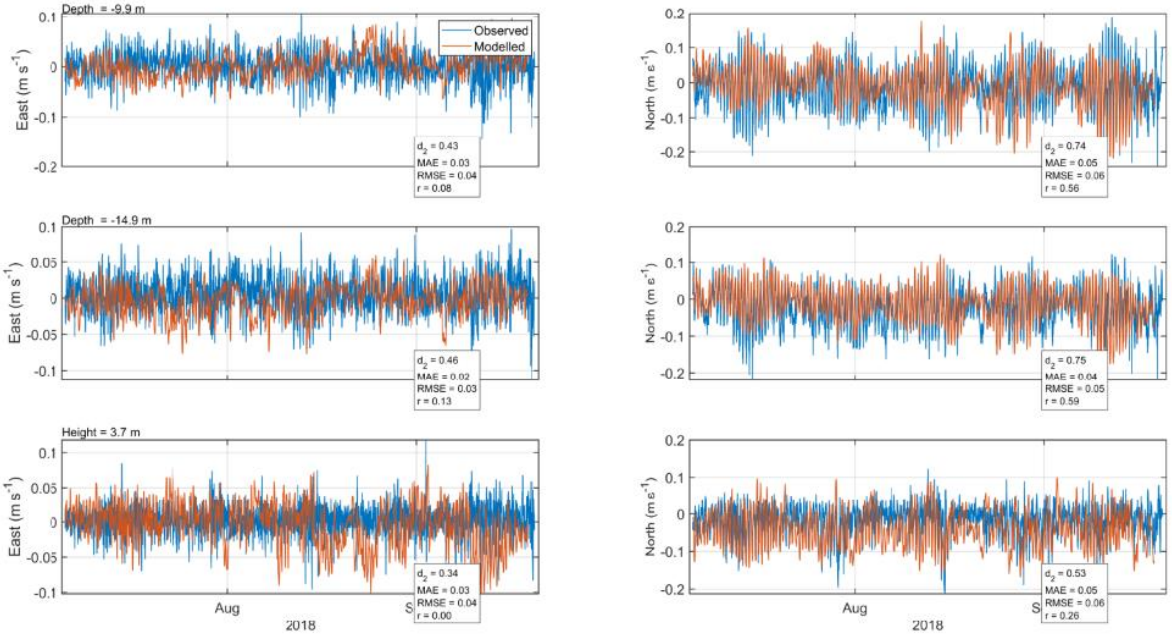

Figure 14. Comparison between observed and modelled East (left) and North (right) components of velocity at the three selected cell depths at the ADCP location for 15 days in July – September 2018 (ID230). Observed data are in blue, model results in red.

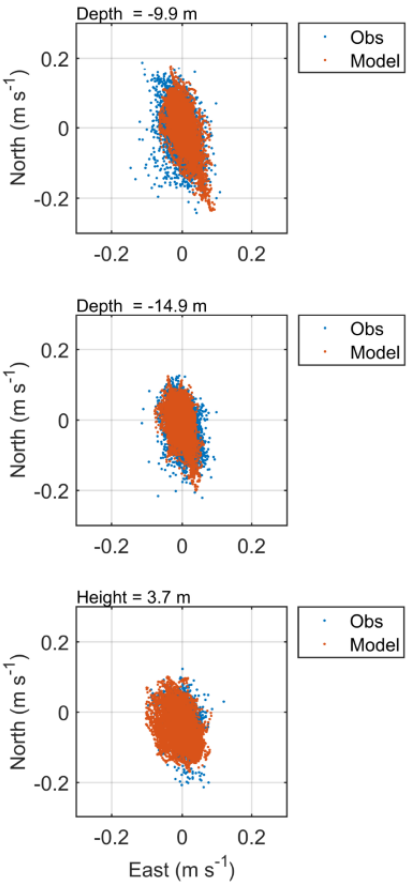

Figure 15. Scatter plot of observed and modelled velocity at each of the three selected cell depths at the ADCP location from July – September 2018 (ID230). Observed data are in blue, model results in red.

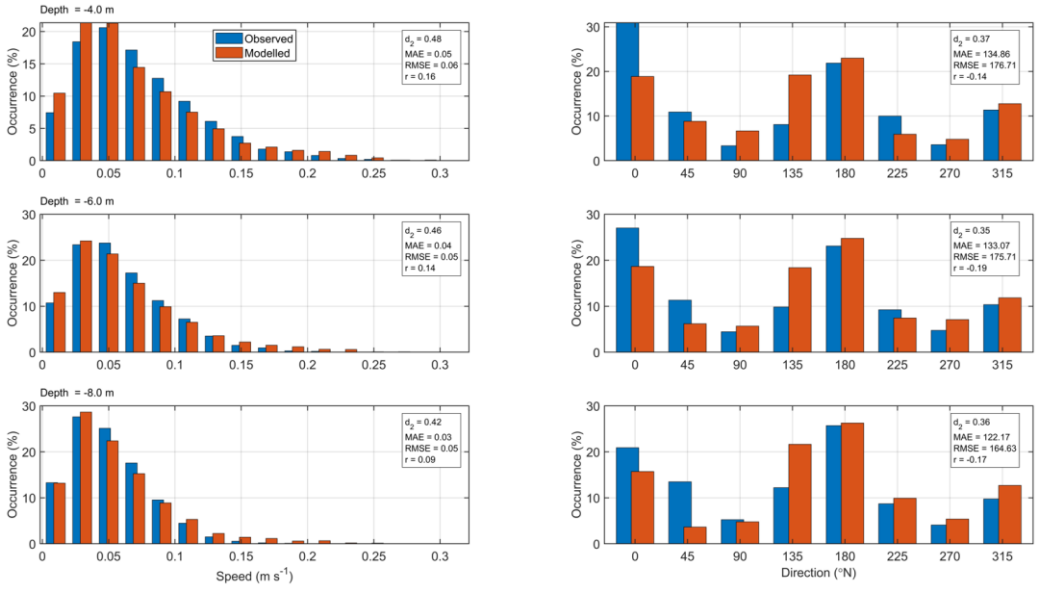

Figure 16. Histograms of observed and modelled speed (left) and direction (right) at the three selected cell depths at the ADCP location from July – September 2018 (ID230). Observed data are in blue, model results in red.

3.4 Validation: April – July 2025, ID448

The model was then validated for a third time using the data collected at the Maol Ban site in April 2025. It used observed depth and current velocity from the ADCP location to compare with modelled sea surface height (SSH) and velocity. The model was validated again by using the same parameters as above.

The results of the validation exercise are presented in Figure 17 - Figure 20 and Table 5. At the ADCP location, the sea surface height was reasonably accurately modelled, with model skill of 1. The mean absolute error (MAE) and root-mean-square error (RMSE) values of 0.14 m and 0.17 m are about 2.5 % and 3.05 % of the spring tide range (5.58 m) respectively.

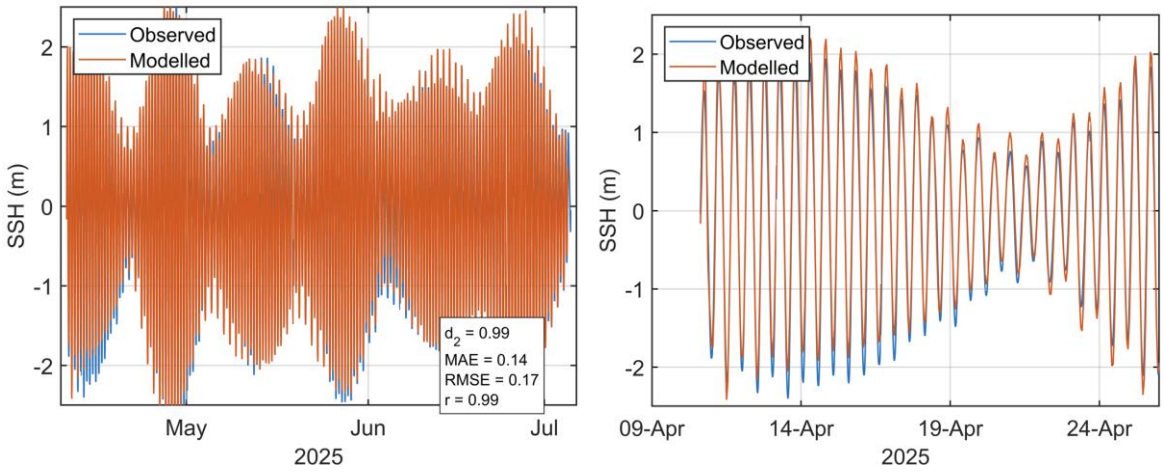

Figure 17. Comparison between observed and modelled sea surface height from April – July 2025 (ADCP deployment ID448) using model parameter values from Table 1. Both the full record (left) and a subset of 15 days (right) are shown. Observed data are in blue, model results in red.

For the validation period, the model skill scores for the East component were 0.45, 0.37 and 0.44 at the three selected cell depths. For the North component of velocity, the model skill scores were 0.76, 0.81 and 0.61 at the three selected cell depths. MAE and RMSE values were between 0.02 and 0.05 for the two velocity components at the three cell depths (Table 5, Figure 18). The scatter plots and histograms demonstrate that the modelled current had broadly the same magnitude and direction characteristics as the observed data (Figure 11 and Figure 12). The modelled near-bed currents are weaker than the observed, but since bath medicine dispersion occurs in the near-surface layers, where the comparison was better, the weaker near-bed currents are unlikely to impact the bath medicine dispersion simulations.

Table 5. Model performance statistics for East and North velocity at the ADCP location from April – July 2025 (ID448) for the three selected cells.

		East	North
Near-surface cell	Model skill	0.45	0.76
	MAE	0.03	0.04
	RMSE	0.03	0.05
Cage-bottom cell	Model skill	0.37	0.81
	MAE	0.02	0.03
	RMSE	0.03	0.04
Near-bed cell	Model Skill	0.44	0.61
	MAE	0.02	0.04
	RMSE	0.03	0.05

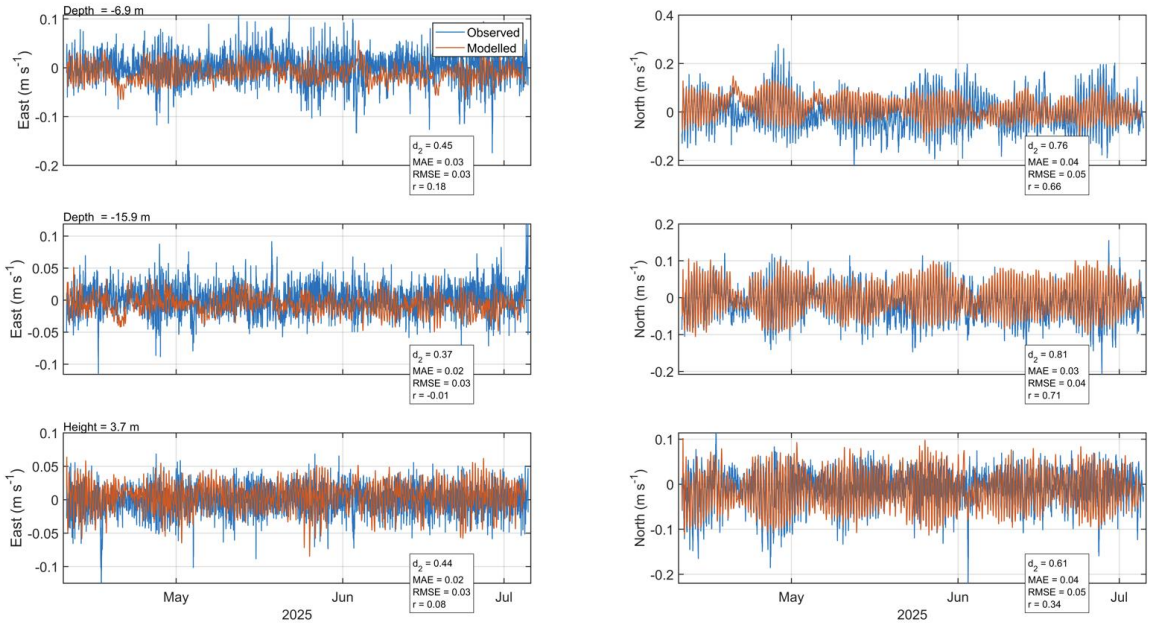

Figure 18. Comparison between observed and modelled East (left) and North (right) components of velocity at the three selected cell depths at the ADCP location for 15 days in April – July 2025 (ID448). Observed data are in blue, model results in red.

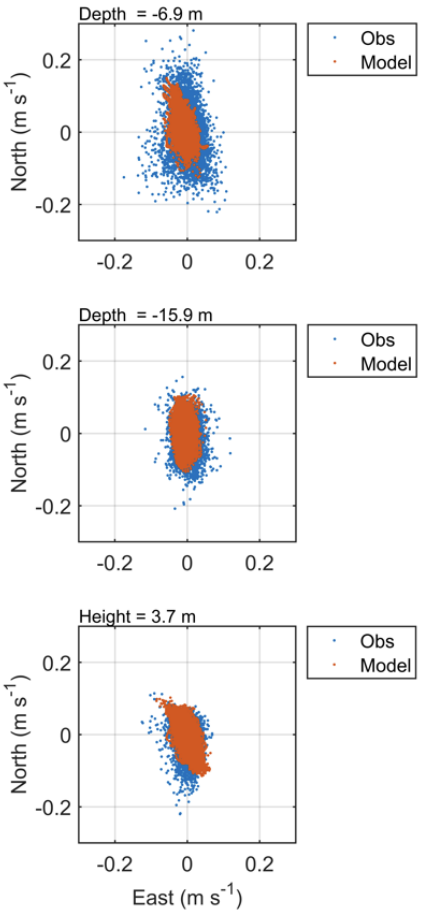

Figure 19. Scatter plot of observed and modelled velocity at each of the three selected cell depths at the ADCP location from April – July 2025 (ID448). Observed data are in blue, model results in red.

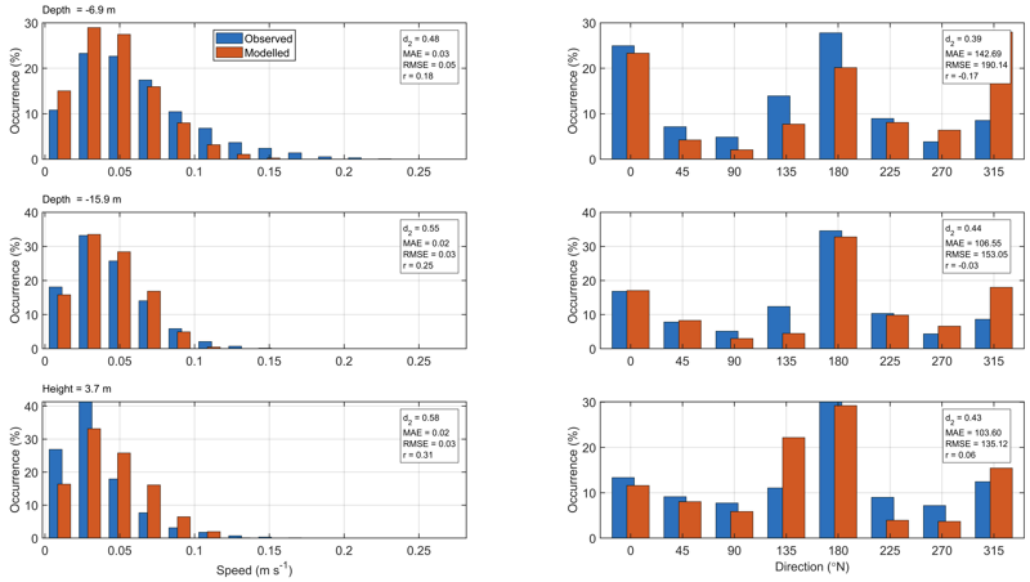

Figure 20. Histograms of observed and modelled speed (left) and direction (right) at the three selected cell depths at the ADCP location from April – July 2025 (ID448). Observed data are in blue, model results in red.

4. Modelled Flow Fields, March – June 2024 (ID437)

Modelled flood and ebb velocity vectors at a spring tide on 5th April 2024 are illustrated in Figure 21. Mean current speeds are moderate around the Cairidh and Maol Ban sites, with a mean current speed of about 5 cm s^{-1} and 7 cm s^{-1} respectively. Figure 22 shows the surface streamlines around the sites at both ebb and flood tides.

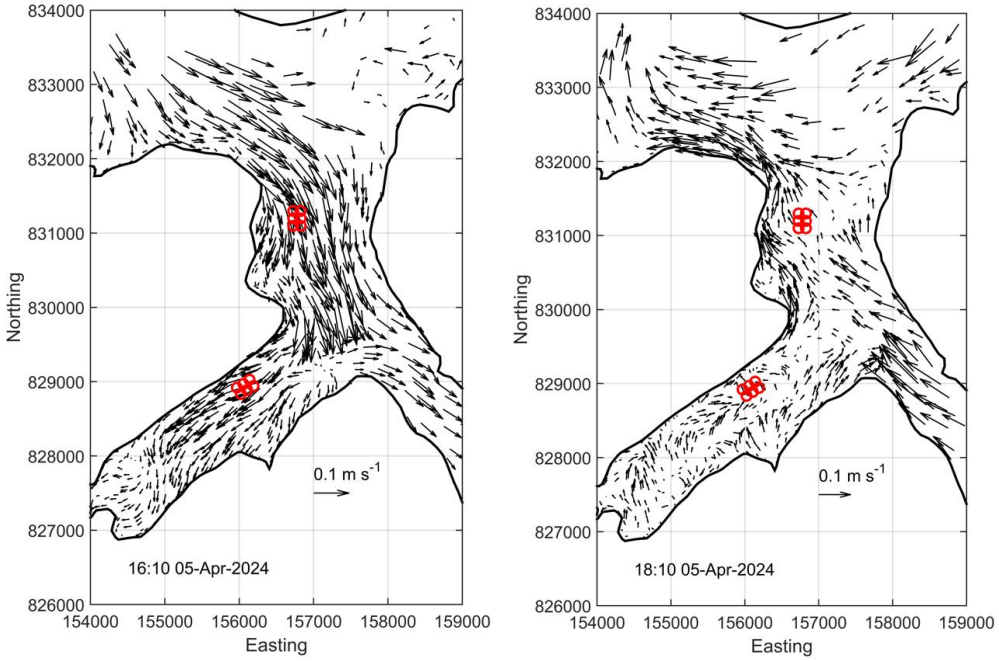

Figure 21. Modelled flood (left) and ebb (right) surface current vectors during spring tides. For clarity, only every 10th vector is shown.

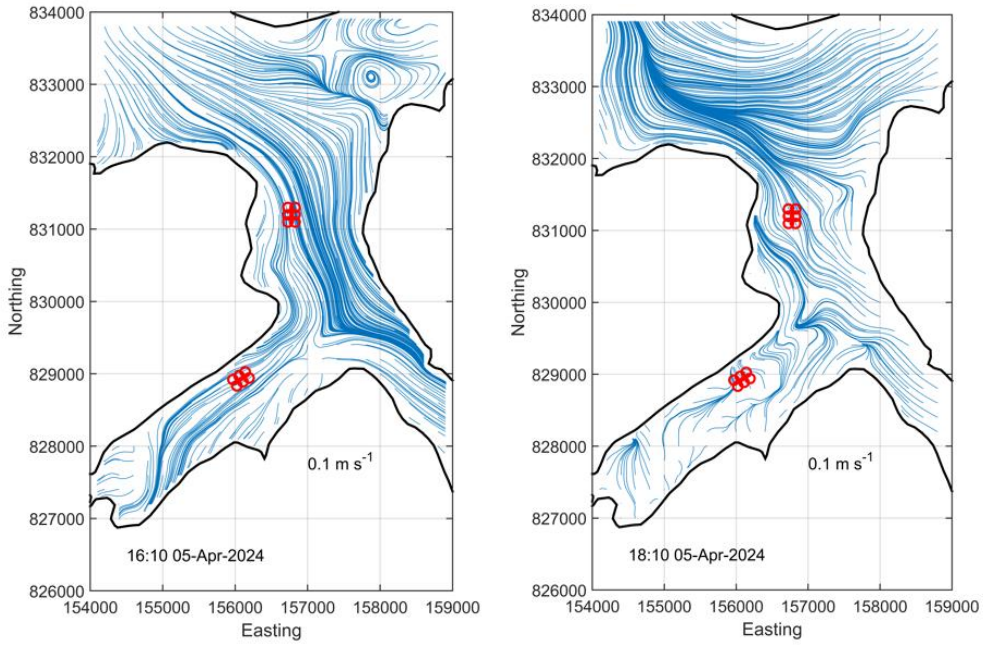

Figure 22. Modelled flood (left) and ebb (right) surface streamlines during spring tides.

5. Model Evaluation against Dye and Drogue Track Data

Anderson Marine Surveys Ltd. undertook a number of dye and drogue studies at the Cairidh and Maol Ban sites between 1st and 4th March 2022.

5.1 Dye Releases

Following each release, multiple discrete surveys of the dye patch were undertaken. From these data, the location of the centre of the dye patch was estimated over time. The times and locations of the dye releases are detailed in Table 6 and Table 7 respectively. For each release, 1 kg of dye was discharged.

The modelling simulated these releases by releasing particles in discrete patches at the times given in Table 6 and Table 7. Modelled particle locations were recorded every 10 minutes, and the mean particle location (assumed to represent the centre of the patch) was calculated. Particles were released in a 10 m radius circle about the release location over a depth range of 0 – 1 m. The tracks of the modelled particle patch centres (calculated as the mean location of all particles) were then compared to the observed data tracks.

Table 6. Details of the dye releases undertaken at Cairidh in March 2022

Release	Date	Release Time	Easting	Northing
1A	01/03/2022	07:48:25	156439	829232
1B	01/03/2022	10:41:00	156409	829384
1C	01/03/2022	15:15:55	156554	829162
2	02/03/2022	07:16:00	156405	829227
3	02/03/2022	09:21:20	156438	829229
4	02/03/2022	13:16:30	156451	829241

Table 7. Details of the dye releases undertaken at Maol Ban in March 2022

Release	Date	Release Time	Easting	Northing
5	03/03/2022	07:23:10	156780	830602
6	03/03/2022	09:14:10	156783	830616
7	03/03/2022	11:30:50	156772	830607
8	03/03/2022	14:45:10	156789	830556
9	03/03/2022	16:55:40	156770	830499
10A	04/03/2022	07:06:05	156777	830514
10B	04/03/2022	10:28:15	156391	830642
10C	04/03/2022	15:58:30	156373	830939

The modelled dye tracks broadly match the tracks of the observed dye releases, with the exception of the 10B release from Maol Ban (shown in blue) which travelled much further than the observed dye patch, and releases 8 & 9 which travelled in the opposite direction to the observed (Figure 23). The vector and streamline plots in Figure 21 and Figure 22 highlight the complexity of the hydrodynamics around the two sites. There are random eddying effects and strong streamline currents throughout the domain which can make prediction of the subsequent dye tracks more challenging as the initial movements can significantly affect subsequent displacement. For the other releases at both sites, the modelled tracks are good, generally reproducing both the direction and magnitude of travel.

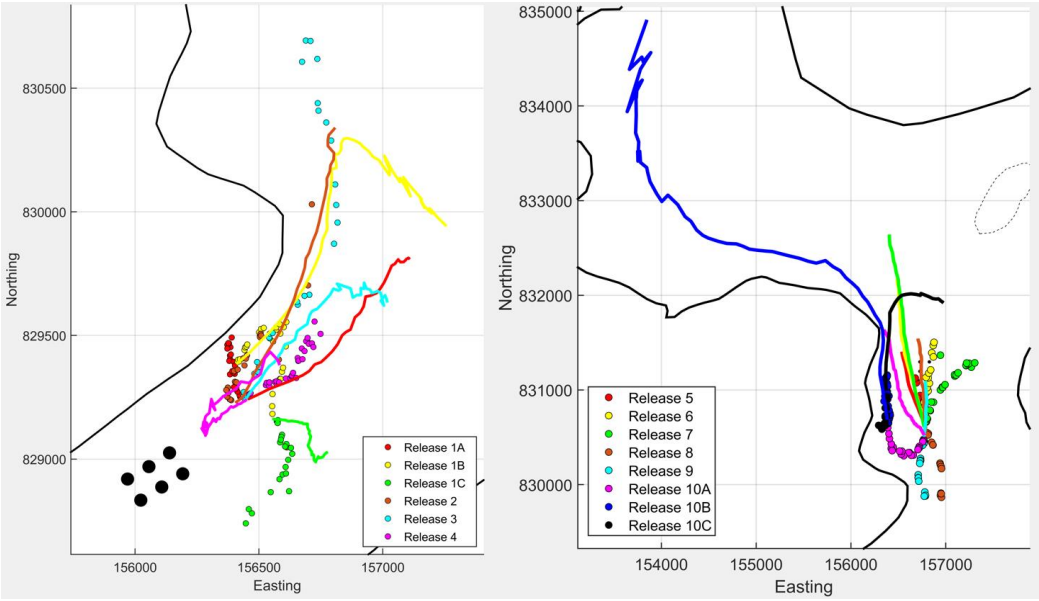

Figure 23. Observed (symbols) and modelled (solid lines) dye release tracks at Cairidh (left) and Maol Ban (right).

5.2 Drogue Releases

The drogue releases were carried out alongside the dye releases, using standard-pattern drogues with a reduced sail depth (≈1 m, due to relatively shallow water depths), fitted with GlobalSat GPS dataloggers recording at 2 min intervals. Three drogues were used at each release, details of the release times and locations are given in Table 8, Table 9, Table 10 and Table 11. *Note that the drogue release numbers do not correspond directly to the dye release numbers.*

Table 8. Details of the drogue releases undertaken at Cairidh in March 2022. Note that the drogue release numbers do not correspond directly to the dye release numbers.

Release No.	Date	Release Time	Recovery Time	Duration (hrs)
1	01/03/2022	07:47	18:20	10:33
2	02/03/2022	07:14	09:15	02:01
3	02/03/2022	09:20	10:32	01:12
4	02/03/2022	10:52	11:55	01:03
5	02/03/2022	12:03	13:58	01:55
6	02/03/2022	14:04	15:40	01:36
7	02/03/2022	15:46	17:32	01:46

Table 9. *Details of the drogue releases undertaken at Maol Ban in March 2022. Note that the drogue release numbers do not correspond directly to the dye release numbers.*

Release No.	Date	Release Time	Recovery Time	Duration (hrs)
8	03/03/2022	11:30	14:30	03:00
9	03/03/2022	14:43	16:44	02:01
10	03/03/2022	16:54	18:15	01:21
11	04/03/2022	07:04	18:10	11:06

The modelling simulated the drogue releases similar to that of the dye patches - by releasing particles in discrete patches at the times given in Table 8 and Table 9. Modelled particle locations were recorded every 10 minutes, and the mean particle location (assumed to represent the drogue location) was calculated. Particles were released in a 10 m radius circle about the release location over a depth range of 0 – 1 m. The tracks of the modelled drogues (calculated from the mean particle location for each release) were then compared to the observed data tracks.

Figure 24 shows the modelled and observed drogue tracks for the releases detailed in Table 10 and Table 11. The drogue releases at Cairidh confirm that the model broadly matches the tracks of the observed drogues. Release 8 at Maol Ban broadly matches the direction and distance of the observed with a slight offset but Releases 9, 10 and 11 show some variability. It is assumed that again, due to the complexity of the hydrodynamics in this area shown in Figure 21 and Figure 22, that the drogue tracking predictions are more challenging as the initial movements can significantly affect subsequent displacement.

Table 10. Location details for each drogue release from Cairidh

Release No.	Drogue No.	Easting	Northing
1	i	156433	829277
1	ii	156433	829285
1	iii	156433	829278
2	i	156393	829264
2	ii	156356	829290
2	iii	156355	829287
3	i	156442	829239
3	ii	156429	829248
3	iii	156432	829233
4	i	156435	829265
4	ii	156436	829253
4	iii	156456	829271
5	i	156439	829263
5	ii	156447	829233
5	iii	156453	829216
6	i	156442	829207
6	ii	156438	829212
6	iii	156434	829240
7	i	156440	829201
7	ii	156430	829212
7	iii	156417	829234

Given the challenges in modelling short-term dye and drogue tracks in dynamic tidal environments, the comparison shown here between modelled and observed tracks for both dye and drogue releases is considered to be acceptable, and demonstrates that the hydrodynamic model is capable of providing good predictions of transport pathways and dispersion of wastes discharged into the local marine environment.

Table 11. Location details for each drogue release from Maol ban

Release No.	Drogue No.	Easting	Northing
8	i	156806	830580
8	ii	156834	830644
8	iii	156798	830594
9	i	156774	830540
9	ii	156803	830546
9	iii	156803	830564
10	i	156785	830501
10	ii	156752	830509
10	iii	156752	830509
11	i	156817	830376
11	ii	156800	830483
11	iii	156819	830386

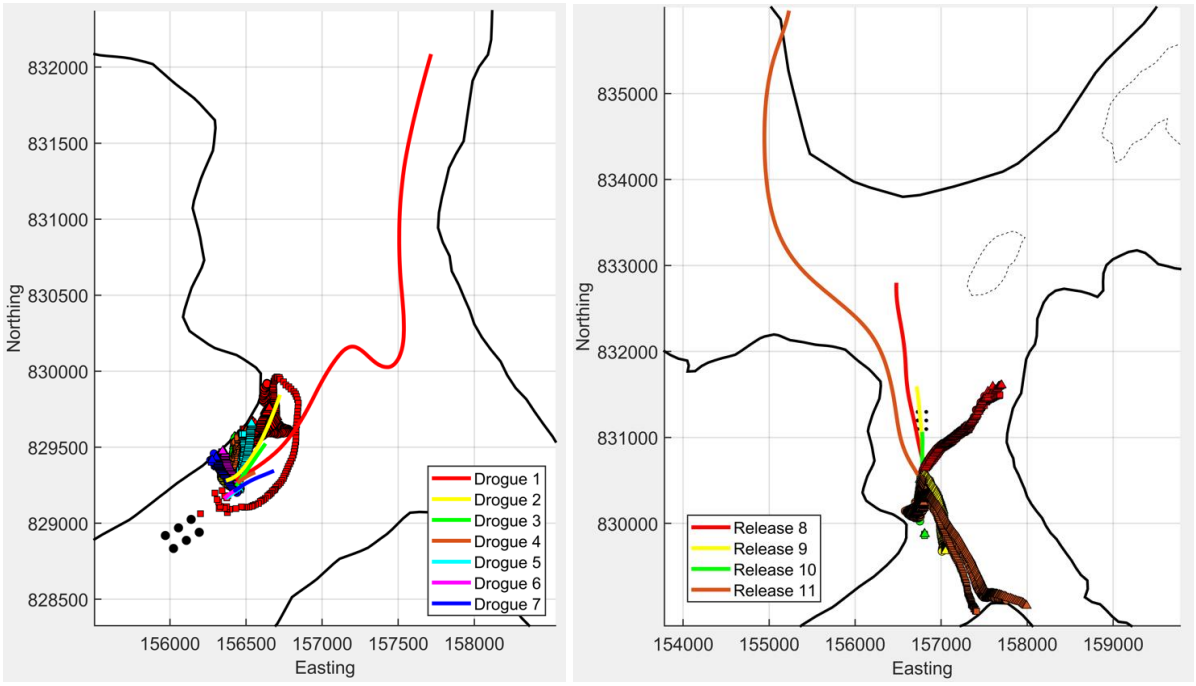

Figure 24. Observed (symbols) and modelled (solid lines) drogue tracks from the releases at Cairidh (left) and Maol Ban (right) from the 1st – 4th March 2022. The different shaped symbols represent individual drogues.

6. References

ECMWF, 2021. ERA5 Dataset, European Centre for Medium-Range Weather Forecasts, https://www.ecmwf.int/en/forecasts/datasets/reanalysis-datasets/era5

Marine Scotland, 2016. Scottish Shelf Model. Part 1: Shelf-Wide Domain. Available at http://marine.gov.scot/taxonomy/term/1964#:~:text=The%20Scottish%20Shelf%20Model%20%20%20%20,%20%20%20%2016%20more%20rows%20

Mowi, 2025a. Azamethiphos Dispersion Modelling Report: Cairidh, Caol Mor. Mowi Scotland Ltd., April 2025, 28 pp.

Mowi, 2025b. Azamethiphos Dispersion Modelling Report: Maol Ban Caol Mor. Mowi Scotland Ltd., April 2025, 28 pp.

Pawlowicz, R.; Beardsley, B.; Lentz, S., 2002. Classical tidal harmonic analysis including error estimates in MATLAB using T_TIDE. Computers & Geosciences, 28, 929-937.

SEPA, 2023. Interim Marine Modelling Guidance for Aquaculture Applications. Scottish Environment Protection Agency, December 2023, 11 pp.

Walters, R.A.; Casulli, V., 1998. A robust, finite element model for hydrostatic surface water flows. Comm. Num. Methods Eng., 14, 931–940.

Willmott, C. J.; Ackleson, S. G.; Davis, R. E.; Feddema, J. J.; Klink, K. M.; Legates, D. R. O'Donnell, J.; Rowe, C. M. 1985. Statistics for evaluation and comparison of models, J. Geophys. Res., 90, 8995– 9005.